INSTITUTE FOR NUCLEAR STUDY
UNIVERSITY OF TOKYO
Tanashi, Tokyo 188
Japan

INS-Rep.-713
Oct. 1988

CHROMIUM AND TITANIUM ISOTOPES PRODUCED IN PHOTONUCLEAR REACTIONS OF VANADIUM, REVISITED

K. SAKAMOTO, M. YOSHIDA, Y. KUBOTA, T. FUKASAWA, A. KUNUGISE AND Y. HAMAJIMA

Department of Chemistry, Faculty of Science, Kanazawa University, Kanazawa 920, Japan

S. SHIBATA

Institute for Nuclear Study, University of Tokyo, Tanashi, Tokyo 188, Japan

I. FUJIWARA

Ottemon Gakuin University, Ibaragi, Osaka 567, Japan

INS-Rep.-713
Oct. 1988

CHROMIUM AND TITANIUM ISOTOPES PRODUCED IN PHOTONUCLEAR REACTIONS OF VANADIUM, REVISITED

K. SAKAMOTO, M. YOSHIDA, Y. KUBOTA, T. FUKASAWA, A. KUNUGISE AND Y. HAMAJIMA

Department of Chemistry, Faculty of Science, Kanazawa University, Kanazawa 920, Japan

S. SHIBATA

Institute for Nuclear Study, University of Tokyo, Tanashi, Tokyo 188, Japan

I. FUJIWARA

Ottemon Gakuin University, Ibaragi, Osaka 567, Japan

Abstract: Photonuclear production yields of ^{51}Ti and ^{51,49,48}Cr from ^{51}V were redetermined for bremsstrahlung end-point energies (E_0) of 30 to 1000 or 1050 MeV with an aid of radiochemical separation of Cr. The yield curves for ^{51}Ti, ^{51}Cr, ^{49}Cr and ^{48}Cr show a clear evidence for two components ; one for secondary-proton reaction at $E_0 < Q_\pi \pm$ and the other for photopion reaction, at $E_0 > Q_\pi \pm$, $Q_\pi \pm$ being Q values for (γ, π^+) and $(\gamma, \pi^- xn)$-reactions. The contributions of the

secondary reactions for production of the Ti and Cr isotopes at $E_0 > Q_{\pi^\pm}$ were then estimated by fitting a calculated secondary yields to the observed ones at $E_0 < Q_{\pi^\pm}$, and found to be about 40, 20, 4 and 4% for ^{51}Ti, ^{51}Cr, ^{49}Cr and ^{48}Cr, respectively, at E_0=400 to 1000 MeV. The calculation of the secondary yields was based on the excitation functions for ^{51}V(n,p) and (p,x'n) calculated with ALICE code and the reported photoneutron and photoproton spectra from ^{12}C and some other complex nuclei.

The present results for ^{49}Cr are very close to the reported ones, while the present ^{48}Cr yields differ by a factor of about 50. For the ^{51}Ti and ^{51}Cr yields, there are some discrepancies between the present and reported ones. The yields corrected for the secondaries, in unit of μb/equivalent quantum, were unfolded into cross sections per photon, in unit of μb, as a function of monochromatic photon energy with the LOUHI-82 code. The results for the ^{51}Ti and ^{49}Cr are in disagreement in both the magnitude and shape with the theoretical predictions based on DWIA and PWIA. A Monte Carlo calculation does not reproduce the present result for the ^{49}Cr yield.

1. Introduction

Photopion reactions have received great interest in view of the Δ formation in electromagnetic nuclear interaction and behaviors of the excited nucleon (Δ) and its decay products

(pion and nucleon) in the nucleus, and have been extensively studied so far. However, the study has rather restricted to yield measurements of the most simple type of $(\gamma,\pi^{\pm})$ reactions or to measurements of emitted pions or nucleons (N) in $(\gamma,\pi N)$ or (γ,N) reaotions. The radiochemical method is suited to determine the product yields of the (γ,π^{+}) and $(\gamma,\pi^{-}xn)$ with $x\geq 0$, selectively from the spallation products dominated in an irradiation with bremsstrahlung beam of continuous spectrum. Extensive radiochemical studies of $(\gamma,\pi^{-}xn)$ reactions with x>1 have been existed on ^{51}V for x=3 (^{48}Cr) by di Napoli et al. (1978)[1]), for x=2 (^{49}Cr) by Meyer and Hummel(1965)[2]), Nydahl and Forkman (1968)[3]), Kumbartzki and Kim (1971)[4]), Bülow et al.(1976)[5]), Blomqvist et al. (1976)[6]) and di Napoli et al. (1978)[1]) and for x=0 (^{51}Cr) by Blomqvist et al. (1977)[7]). For radionuclide yields from (γ,π^{+}), reported examples included measurements of ^{51}Ti from ^{51}V [refs. [3,7,8]) and refs. therein also for other nuclides]. Radionuclide measurements for $(\gamma,\pi^{-}xn)$ on some other targets such as ^{197}Au have been reported less extensively[9,10,11]).

The present article reports determinations of $^{51,49,48}Cr$ produced by $^{51}V(\gamma,\pi^{-}xn)$ and of ^{51}Ti by $^{51}V(\gamma,\pi^{+})$ reactions for bremsstrahlung end-point energies (E_0) of 30 to 1000 MeV. A cursed problem in radiochemical method is the presence of non-mesic interaction ; secondary protons and neutrons lead the same products of $(\gamma,\pi^{-}xn)$ and (γ,π^{+}) reactions through (p,x'n) and (n,p) reactions, respectively. An emphasis in the present work

was placed on runs around and below thresholds for pion production to asses the contribution of the interfering processes.

2. Experimental

Three high-purity (99.9%) vanadium metal plates (16.4 mg/cm^2) and one disk (600 mg/cm^2) of reagent-grade vanadium oxide were stacked and placed in a quartz tube together with aluminum monitor foils of 6.6 mg/cm^2 and/or gold monitor foils of 80 mg/cm^2 and irradiated for 5 min in a water-cooled target holder with uncollimated bremsstrahlung beam of end-point energies of E_0=30 to 210 MeV from the 300 MeV electron linac of the Laboratory of Nuclear Science (LNS), Tohoku University[12]. The natural vanadium used as the target material is practically monoisotopic (99.76% for ^{51}V). A V_2O_5 disk of 600 mg/cm^2 sandwiched with a metallic vanadium plate of 150 mg/cm^2 and an aluminum monitor plate of 270 mg/cm^2 was irradiated for 30 min in air with collimated electron-free bremsstrahlung of E_0=300 to 1000 or 1050 MeV from the 1.3 GeV Electron Synchrotron of the Institute for Nuclear Study (INS), University of Tokyo. The beam intensity was monitored with a Wilson-type thick chamber counter at INS, but the photon-intensity used in the yield calculation for $E_0 \geq 100$ MeV was obtained from the monitor reaction ^{27}Al(γ,2pn)^{24}Na [ref.[13])] and that for $E_0 \leq 65$ MeV was

from $^{197}Au(\gamma,n)^{196}Au$ [refs.[14,15])]. After irradiation, the V_2O_5 target was dissolved in presence of Cr^{3+} carrier with 20 ml of 6N NaOH and a few ml of H_2O_2, and the solution was adjusted to pH 2 with H_2SO_4. Chromium was then extracted from the ice-cooled solution into a cooled mixture of 50 ml of ethylacetate and 2 ml of H_2O_2, back-extracted into 2N KOH, and precipitated as $BaCrO_4$ by adding $BaCl_2$ to the slightly acidic solution under presence of CH_3COOH. Gamma-ray measurements with high-purity Ge detectors of 1.6 to 1.7 keV resolution were performed on the $BaCrO_4$ on a cellulose nitrate membrane filter and the metals of V, Al and/or Au from the same irradiation. The photopeak assignment was based on energy and half-life, and the detector efficiency was determined with a calibrated ^{152}Eu source of the same size as the sample. The relevant nuclear data[16,17]) are shown in table 1. All the ^{51}Ti yields and most of the ^{49}Cr yields were obtained from the metal targets non-destructively. The chemical yields were determined gravimetrically and also from comparison of photopeak counts with those of the metal target of the same irradiation.

3. Results and Discussion

The measured yields in μb per equivalent quanta are given in table 2. The results obtained from the multiplicate measurements are listed separately, along with the chemical

yields. The attached errors are mostly due to counting statistics. Only an upper limit is given to ^{49}Cr at E_0=30 and 45 MeV and to ^{48}Cr at E_0=30, 45 and 65 MeV. The present results (circles) are compared with the reported data (open triangles, closed diamonds and closed circles) in figs. 1(a) to 1(d) for the studied E_0 range in the present work. Arrows with $Q_p^{52-x'}$, Q_n^{51} and $(Q^{51-x})_{\pi^\pm}$ on the E_0 axis show the Q values for ^{51}V(p,x'n), ^{51}V(n,p) and ^{51}V($\gamma,\pi^\pm$xn), respectively. Note that Q_p and Q_n are the particle energies calculated from mass excess[17]) and are indicated on the E_0 axis for convenience. Some scatters in the present data are originated in low chemical yields of several to 10% obtained in an early stage of the present work, and the solid curves noted as $(^{51-x}Cr)_{obs}$ in the figures are drawn for eye-guide through the data points, favoring those with high chemical yields of about 30 to 60% (see table 2). It is noted that the yields at E_0=30 to 195 or 220 MeV (±3~5%) measured at the LNS linac are smoothly connected with those at E_0=300 to 1000 or 1050 MeV (±0.3%) measured at the INS synchrotron.

The E_0 variation of the observed ^{51}Cr yields, $(^{51}Cr)_{obs}$, shows clearly that there exist two components ; one is from the photopion reaction, $(^{51}Cr)_{\pi^-}$, and the other from the secondary proton reaction, $(^{51}Cr)_p$. The threshold for the latter reaction is consistent with Q_p^{51}. Though the ^{51}Cr production below $(Q^{51})_{\pi^-}$ is considered to be produced purely by the secondary proton reaction, the secondary reaction is superposed upon by the

(γ,π^-) reactions above $(Q^{51})_{\pi^-}$. The contribution of the secondary reaction to the observed ^{49}Cr production is about 20% at $E_0>300$ MeV, as indicated with the broken curve noted as $(^{51}Cr)_p$ in fig. 1(a). The $(^{51}Cr)_p$ was estimated on the basis of the reported photoproton at 40° from ^{12}C[ref.^{18})] and at 72° from ^{12}C[ref.^{19})] and some other complex nuclei[20]) and the excitation function for $^{51}V(p,n)$ reaction up to E_p=90 MeV calculated with the ALICE code[21,22]). For $E_p \geq 90$ MeV, we have assumed that the cross section decreases exponentially, i.e. $\sigma(90\ \text{MeV})\cdot\exp(-\underline{a}E_p)$, $\underline{a}$ being an adjustable parameter obtained by fitting to the ALICE results at $E_p \leq 90$ MeV, $\sigma(\leq 90$ MeV). The cross section measurements of the $(^{51}V+p)$ reaction are best available for (p,n)[23,24]), and the agreement of the ALICE results with the measured ones, especially in shape, is fairly good. The reported photoproton spectra at high energies were assumed to be isotropic for a heavier target under study and origined in quasideuteron mechanism with the Levinger constant L=5~13[18]). Those at low energies were not available, and were estimated by fitting the calculated ^{51}Cr yields to those observed below $(Q^{51})_{\pi^-}$, assuming that they are entirely from the secondary-proton reaction, $^{51}V(p,n)^{51}Cr$. Subtraction of the $(^{51}Cr)_p$ from the observed yields results in the net yields which are shown by the dotted curve that starts from $(Q^{51})_{\pi^-}$. The net yields are regarded to be from $^{51}V(\gamma,\pi^-)$ reaction, and indicated as $(^{51}Cr)_{\pi^-}$.

The reported results for $(^{51}Cr)_{\pi^-}$ by Blomqvist et

al.[7])(triangles) are in agreement with the present results $(^{51}Cr)_{\pi^-}$ around the threshold and at 500 MeV, but deviate largely in between.

The observed yields of ^{49}Cr in fig. 1(b) also show the two-component variation. The contribution of $(^{49}Cr)_p$ from $^{51}V(p,3n)$ reaction (dashed curve) was estimated by the same method and parameters as described above for ^{51}Cr, and found to amount only to 3.4~4.5% of the observed yields at E_0>300 MeV. The calculated excitation function for $^{51}V(p,3n)^{49}Cr$ was proved to be consistent with the measured ones at E_p=60 to 240 MeV by Heininger and Wiig[25]).

Bülow et al. (1976)[5]) noted that their yield values of ^{49}Cr for E_0=200 to 800 MeV were consistent within the experimental errors with the earlier results for E_0=1000 to 2100 MeV by Kumbartzki and Kim[4]) and for $E_0 \leq 750$ MeV by Nydahl and Forkman[3]) when the latters were corrected with a revised gamma-branching ratio. Also the values obtained for E_0=300 to 1000 MeV by di Napoli et al.[1]) were not indistinguishable from those by Bülow et al.[5]). These earlier results, all of which are shown by closed circles in fig. 1(b), show a slower increase with increase of E_0 than the present ones, approaching our $(^{49}Cr)_{obs}=(^{49}Cr)_p + (^{49}Cr)_{\pi^-}$, rather than $(^{49}Cr)_{\pi^-}$, at $E_0 \geq 900$ MeV. Blomqvist et al.[6,7]) stated that special care was taken in their measurements of $(\gamma,\pi^{\pm})$ and $(e,e'\pi^{\pm})$ reactions on ^{27}Al and ^{51}V to subtract out the background yields due to secondaries. Their results on ^{49}Cr for E_0=150 to 575 MeV[6]) shown by open triangles in fig. 1(b)

are more closer to the present ones than the previous results mentioned above are. The present measurement was not extensive enough in the E_0 range of 200 to 300 MeV, the range of the most importance in the later discussion, but the results appear to be very close to but slightly different in shape from the earliest and extensive measurement at E_0 from threshold to 300 MeV by Meyer and Hummel (1965)[2]. Their results in unit of reactions per MeV per (mole/cm^2) were converted to those in unit of μb/eq.q. and shown by closed diamonds in fig. 1(b). All the reported data in fig. 1(b) have been corrected more or less for the background $(^{49}Cr)_p$ by the previous investigators, and must be compared with the present result shown by the dotted curve, $(^{49}Cr)_{\pi^-}$, but not by the circles nor the solid curve $(^{49}Cr)_{obs}$. All the reported data at E_0<200 MeV suggest still insufficient correction of the background. It should also be pointed out here that Kumbartzki and Kim[4] and di Napoli et al.[1] used the monitor reaction $^{27}Al(\gamma,2pn)^{24}Na$, absolute yields of which were calibrated with quantameters by themselves, but the values by the later investigators[7] differed systematically by 20% from those by Johnsson et al.[13] which was used in the present work. The value at E_0=850 MeV by Johnsson et al. was confirmed to be consistent within our experimental uncertainty of 15% with the measurement by the INS quantameter [see ref.[15]) for monitor reactions].

In fig. 1(c), the results for ^{48}Cr are presented. The contribution of the secondary protons, $(^{48}Cr)_p$, was estimated to

be such an extent as shown by the dashed curve. This estimation for $(^{48}Cr)_p$ was performed in the same manner as above for $(^{51}Cr)_p$ and $(^{49}Cr)_p$. A poor agreement of the calculated proton cross sections with the measured ones at E_p=60 and 100 MeV by Heininger and Wiig[25]) was found, and the estimation of $(^{48}Cr)_p$ was solely based on the ALICE result. The contribution of the $(^{48}Cr)_p$ to the observed yields becomes to be 2.6~5.2% at $E_0 \geq 400$ MeV, being about the same as for ^{49}Cr. The ^{48}Cr yields in the present work are lower by a factor of 50 than those reported for E_0=300 to 1000 or 1050 MeV by di Napoli et al.[1])(closed circles). This discrepancy can not be accounted for, but it seems unlikely that (γ,π^-2n) reaction is far less probable than (γ,π^-3n) reaction on these medium-weight targets[26]).

The observed yield profile for ^{51}Ti [fig.1(d)] is similar to that for the Cr isotopes, showing a shoulder below Q_{π^+}. The excitation function for $^{51}V(n,p)$ reaction calculated with the ALICE code was used in estimation of $(^{51}Ti)_n$, though the theoretical cross sections were discrepant by a factor of 3 from the reported ones for neutrons of 13 to 19 MeV[27]). The neutron spectrum for E_n>50 MeV was obtained from the measurements by Kaushal et al.[28]) and by von Eyss and Luhrs[29]) and those for E_n<50 MeV were from a fit of the calculated $(^{51}Ti)_n$ to the observed shoulder as the same manner as in the case of the Cr isotopes. The contribution of $(^{51}Ti)_n$ to $(^{51}Ti)_{obs}$ at E_0>300 MeV are about 40%. The ^{51}Ti yields thus obtained for $^{51}V(\gamma,\pi^+)$ reaction, $(^{51}Ti)_{\pi^+}$, are close to but not exactly

agree with the reported ones shown by closed circles for E_0=175~750 MeV by Nydahl and Forkman[3]) and Blomqvist et al.[8]). At 250<E_0<400 MeV, the reported values are in agreement with the present $(^{51}Ti)_{\pi^+}$. And at E_0>400 MeV, the reported ones are rather close to the present $(^{51}Ti)_{obs}=(^{51}Ti)_{\pi^+}+(^{51}Ti)_n$ and both consistent with those (closed squares) for E_0=1 to 2 GeV observed by Kumbartzki and Kim (1971)[4]). An excellent agreement with a more recent result by Blomqvist et al.[7]) (triangles at E_0<600 MeV) was obtained, except at the threshold region. The discrepancy at the threshold might arise in neglect or underestimation of the secondary reaction in the earlier measurements. The difference of the present yield profile of $(^{51}Ti)_{\pi^+}$ from the previous ones is quite similar to those of $(^{49}Cr)_{\pi^-}$. The present data for $(^{51}Ti)_{obs}$ are still crude and a further measurement is required.

Now the yields corrected for the secondaries, $(^{51}Ti)_{\pi^+}$, $(^{51}Cr)_{\pi^-}$, $(^{49}Cr)_{\pi^-}$ and $(^{48}Cr)_{\pi^-}$, have shown to rise steeply after $Q_{\pi^\pm}$ and then to attain roughly constant values, suggesting that photons responsible for production of these product nuclides are mostly of energies lower than 400 MeV. Though there remain some ambiguities due to scattering of the observed yields, the corrected yields in unit of $\sigma_q(E_0)$ were unfolded into cross sections per photon, $\sigma_k(k)$, after the method of Tesch[30]) with an aid of the LOUHI-82 code[31]). In the calculation, the yield values of $\sigma_q(E_0)$ were based on the smoothed ones shown by the dotted curves in fig.1(a)~(d) and the

Schiff spectrum[32]) was used for approximation of bremsstrahlung-production cross section. The results for σ_k are illustrated in fig. 2. Uncertainty in σ_k was estimated from the uncertainty of about 10% in the $(^{49}Cr)_{obs}$ curve to be about 20% at $k \gtrsim 240$ MeV (peak energy) in case of ^{49}Cr and to be larger in cases of the remaining ones. Ambiguity inherited from unfolding process was estimated to be 20 to 30%, depending on choice of the parameter values involved in the code, especially on Gammas's for a measure of smoothing in the calculation. We used 10 and 5 for the two γ values after examining the effect of several choices of the value sets on their reholded results.

It is shown that the four excitation curves are of similar resonant shape with FWHM of 70±5 MeV for ^{51-x}Cr in common and about 80 MeV for ^{51}Ti. The peak energy for ^{51-x}Cr increases rather regularly from 210 to 245 MeV with increase of x from 0 to 3 and the curve for ^{51}Ti locates at k=235 higher than that for ^{51}Cr. Uncertainty in the peak energies was estimated from those originated in unfolding and from a systematics obtained from other targets[26]) to be less than 10%. The ratio of σ_k for ^{51}Cr and for ^{51}Ti, $\sigma_k(\pi^-)/\sigma_k(\pi^+)$ is about 5, which is quite different from a systematic trend of these ratios in terms of averaged cross sections against N/Z in target nucleus found in Monte Carlo calculation and in pion measurements[33,34]).

Theoretical calculations have been available only for ^{51}Ti and ^{49}Cr, as reported by the Lund group[3,5~7]). In fig. 3(a), three calculations for ^{51}Ti (dotted curves I, II and II') are

compared with the three experiments by Nydahl and Forkman[3])(thin line-a), Blomqvist et al.[7]) (thin line-b) and the present work (thick line). One sees how the small discrepancies in $\sigma_q(E_0)$ discussed above result seemingly quite a different $\sigma_k(k)$. The theoretical calculations are on the basis of a valence nucleon model (surface production model) by Nydahl and Forkman[3]) and of an impulse approximation with and without final state interaction (DWIA and PWIA) by Blomqvist et al.[7]). For ^{49}Cr, a Monte Carlo calculation by Bülow et al.[5]) and Blomqvist et al.[6]), who used the Gabriel-Alsmiller program[35]), is entered in comparison with the present result as shown by circled crosses in fig. 3(b). Nydahl and Forkman[3]) also made a calculation for ^{49}Cr by considering that the primary photon interacts with neutrons located both in valence states and inner shells (volume production), and their result (I') is included together with those of the valence nucleon model (I) in fig. 3(b). It is concluded that all the magnitude, peak energy and shape of all the calculations are in disagreement with the experiment. Booth quoted in his review work[36]) a statement by Blomqvist et al.[7]) that the blame is placed on the optical potential which gives too weak an s-wave repulsion and too strong a p-wave absorption.

The total cross sections for $^{51}V(\gamma,\pi^- xn)^{51-x}Cr$ in fig. 2 were obtained by summing those for x=0, 1, 2 and 3. The largest contribution to the total is from $^{51}V(\gamma,\pi^-)^{51}Cr$ and $^{51}V(\gamma,\pi^- n)^{50}Cr$, the excitation curve of the latter was obtained by interpolation of those of $^{51,49,48}Cr$. The total excitation

curve is peaked at k=218 MeV with FWHM of 74 MeV. The peak energy and the magnitude of the total excitation curve for $^{51}V(\gamma,\pi^-xn)^{51-x}Cr$ is much smaller than those expected from (3,3) resonance in pion photoproduction from a free nucleon(N). In fig. 4, the total is compared with the γN cross section, $\sigma_{\gamma N}$[37]), multiplied by 51 (target mass A_t). The latter is a measure for the total absorption cross section of ^{51}V, and for the sum of the various decay channels such as (γ,π^-xn), (γ,π^-xnyp), (γ,π^+xn), (γ,π^+xnyp), (γ,π^0xn), (γ,π^0xnyp) and those without pion emission. The total of (γ,π^-xn) is shown to amount only to 1% of the total absorption, $(51\cdot\sigma_{\gamma N})$. On the other hand, the yield values for $^{51}V(\gamma,spall)$ and $^{51}V(\gamma,\pi^-xn)$ obtained by the present authors[38]) are 45 mb/eq.q. and 0.2 mb/eq.q., respectively, at $E_0\sim1$ GeV. Taking the former into consideration to include spallation induced by photons of energies lower than the Δ-threshold, the ratio of $\sigma(\gamma,\pi^-xn)/\sigma(\gamma,spall)\sim4.4\times10^{-3}$ would reasonably account for the ratio of $\Sigma\sigma_k(\gamma,\pi-xn)/A_t\cdot\sigma_{\gamma N}=1\times10^{-2}$. Fig. 4 indicates that the decay channel for (γ,π^-xn) is actually one of the simplest decay part of (3,3) resonance absorption among others, being opened at the lowest excitation of the resonance absorption. It is also suggested that the photo reaction samples the entire nuclear volume, but the mechanism is not so simple as those described by the old models of surface production nor volume production. A detailed account for consequence of Δ-hole propagation through the nucleus[39]) seems to be required for the

whole picture of the resonance absorption and its decays in the region under consideration.

The authors are indebted to Drs. M. Yagi and K. Masumoto of the Laboratory of Nuclear Science, Tohoku University, and Drs. K. Yoshida, T. Miyachi and M. Mutou of the Institute for Nuclear Study, University of Tokyo, for their invaluable cooperations in accelerator operations and to Mr. T. Unno and the other students of the Radiochemistry Laboratory of Kanazawa University in radioactivity measurements. Miss. N. Fukushima is acknowledged for her typing and drawing. This work was supported by a Grand-in-Aid for Scientific Research (A) (60430012) of the Ministry of Education, Science and Culture of Japan.

References

1) V. Di Napoli, F.Salvetti, M.L.Terranova, H.G.De Carvalho, J.B.Martins and O.A.P.Tavares, J. Inorg. Nucl. Chem. **40** (1978) 175

2) R.A.Meyer and J.P.Hummel, Phys. Rev. 140 (1965) B48

3) G.Nydahl and B.Forkman, Nucl. Phys. B7 (1963) 97

4) G.Kumbartzki and U.Kim, Nucl. Phys. A176 (1971) 23

5) B.Bülow, B.Johnsson, M.Nilsson and B.Forkman, Z. Phys. A278 (1976) 89

6) I.Blomqvist, P.Janeček, G.G.Jonsson, R.Petersson, H.Dinter, K.Tesch, Z. Phys. A278 (1976) 83

7) I.Blomqvist, P.Janeček, G.G.Jonsson, H.Dinter, K.Tesch, N.Freed and P.Ostrander, Phys. Rev. C15 (1977) 988

8) I.Blomqvist, G.Nydahl and B.Forkman, Nucl. Phys. A162

(1971) 193

9) I.Blomqvist, B.Bülow, A.Fredriksen, B.Johnsson, G.G.Jonsson, K.Lindgren, M.Nilsson, R.Petersson, O.Glomset, N.Freed and W.Rhodes, Z. Phys. **A288** (1978) 313

10) B.Bülow, B.Johnsson, G.G.Jonsson, K.Lindgren, M.Nilsson and R.Petersson, Z. Phys. **A290** (1979) 393

11) P.H.Ballentine, J.K.Hersh, H.A.Medicus, S.Planeta, F.Potentiani and S.Rossdeutscher, "Photopion Nuclear Physics", ed. P.Stoler, (1979) p.387

12) K.Sakamoto, H.Toramoto, Y.Hamajima, K.Okada and M.Dohniwa, Radiochim. Acta **37** (1984) 69

13) B.Johnsson, A.Järund and B.Forkman, Z. Phys. **A273** (1975) 97

14) K.Lindgren and G.G.Jonsson, Nucl. Phys. **A166** (1971) 643

15) K.Osada, T.Fukasawa, K.Kobayashi, Y.Hamajima, K.Sakamoto, S.Shibata and I.Fujiwara, Res. Rept. Lab. Nucl. Sci., Tohoku Univ. **20** (1987) 299

16) U.Reus and W.Westmeier, Atomic Data and Nuclear Data Tables, 29 Catalog of Gamma Rays from Radioactive Decay, Pt.II, (1983) p.193

17) E.Browne and R.B.Firestone, "Table of Radioactive Isotopes", ed. V.S.Shirley (John Wily & Sons, N.Y., 1986).

18) G.Andersson, P.Dougan and W.Stiefler, Z. Phys. **A272** (1975) 265

19) J.L.Matthews, W.Bertozzi, S.Kowalski, C.P.Sargent and W. Turchinetz, Nucl. Phys. **A112** (1968) 654

20) P.Dougan, B.Forkman, W.Stiefler and J.L.Matthews, Z. Phys. **269** (1974) 105

21) M.Blann, Ann. Rev. Nucl. Sci. **25** (1975) 123

22) F.Plasil, ORNL Report TM-6054 (1977)

23) G.F.Dell. W.D.Ploughe and H.J.Hausman, Nucl. Phys. **64** (1965) 513 and refs. therein.

24) P.G.Albouy, M.Gusakow, N.Poffé, H.Sergolle and L.Valentin, J. Phys. Radium. **23** (1962) 1000

25) C.G.Heininger and E.O.Wiig, Phys. Rev. 101 (1956) 1074

26) I.Fujiwara, S.Shibata, M.Imanura, M.Soto, Y.Kubota, M.Yoshida, T.Fukasawa, T.Hashimoto, Y.Hamajima and K.Sakamoto, Res. Rep. Lab. Nucl. Sci., Tohoku Univ. 18 (1985) 304

27) M.Bormann, S.Cierjacks, E.Fretwurst, K.J.Giesecke, H.Neuert and H.Pollehn, Z. Phys. 174 (1963) 1

28) N.N.Kaushal, E.J.Winhold, P.F.Yergin, H.A.Medicus and R.H. Augustson, Phys. Rev. 175 (1968) 1330

29) H.J.von Eyss and G.Lührs, Z. Phys. 262 (1973) 393

30) K.Tesch, Nucl. Instr. Meth. 95 (1971) 245

31) J.T.Routti and J.V.Sandberg, Comput. Phys. Commu. 21 (1980) 119

32) L.I.Schiff, Phys. Rev. 83 (1951) 252

33) W.M.McClelland, Phys. Rev. 123 (1961) 1423

34) I.A.Grishaev, A.N.Krinitsyn, N.I.Lapin, V.I.Nikiforov, G.D. Pugachëv and B.I.Shramenko, Sov. J. Nucl. Phys. 14 (1972) 20

35) T.A.Gabriel and R.G.Alsmiller, Jr. Phys. Rev. 182 (1969) 1035

36) E.C.Booth, "Photopion Nuclear Physics", ed. P.Stoler (Plenum Press, N.Y. and London, 1979) p.129

37) Particle Data Group, Phys. Lett. 170B (1986) 85

38) K.Sakamoto, Y.Hamajima, M.Soto, Y.Kubota, M.Yoshida, T. T.Hashimoto, T.Fukasawa, I.Fujiwara and S.Shibata, Res. Rep. Lab. Nucl. Sci., Tohoku Univ. 18 (1985) 290

39) J.H.Koch, E.J.Moniz and N.Ohtsuka, Ann. Phys. 154 (1984) 99 and refs. therein.

Captions of figures

Fig. 1 The yields in unit of μb/equivalent quanta as a function of bremsstrahlung end-point energy E_0. The observed yields in the present work, $(^{51-x}Cr)_{obs}$ and $(^{51}Ti)_{obs}$, are shown by open circles connected with solid lines. The dashed lines indicate the yields from the secondaries, $(^{51-x}Cr)_p$ and $(^{51}Ti)_n$. See text for the secondary yields. The yields from (a)~(c) $^{51}V(\gamma, \pi^-xn)^{51-x}Cr$ for x=0, 2 and 3 and (d) $^{51}V(\gamma,\pi^+)^{51}Ti$ are shown by dotted curves noted with $(^{51}Cr)_{\pi^-}$, $(^{49}Cr)_{\pi^-}$, $(^{48}Cr)_{\pi^-}$ and $(^{51}Ti)_{\pi^+}$, respectively. Comparisons are made with the reported ones ; (a) triangles[7]) for ^{51}Cr, (b) closed diamonds[2]), closed circles[1,3,4,5]) and triangles[6]) for ^{49}Cr, (c) closed circles[1]) for ^{48}Cr and (d) closed circles[3,8]), closed squares[4]) and triangles[7]) for ^{51}Ti. Arrows on E_0 axis show the Q values for $^{51}V(p,x'n)^{51-x'}$, $^{51}V(n,p)^{51}Ti$ and $^{51}V(\gamma,\pi^{\pm}xn)^{51}Ti$ and ^{51-x}Cr.

Fig. 2 Cross sections per photon in unit of μb, σ_k, as a function of photon energy k. The peak energies and (FWHM) are 210(65) MeV for ^{51}Cr, 240(75) MeV for ^{49}Cr, 245(75) MeV for ^{48}Cr and 235(80) MeV for ^{51}Ti. The cross sections for ^{50}Cr from $^{51}V(\gamma,\pi^-2n)$ were obtained from an interpolation and the total (π^-) is the sum of $\sigma_k(\gamma,\pi^-xn)$ for x=0, 1, 2 and 3.

Fig. 3 Comparison of the present σ_k (thick line) with the reported results (thin lines) and theoretical predictions (dotted curves).

(a) for ^{51}Ti : experimental results ; thin line-(a)[3]) and thin line-(b)[7]) and theory ; curve-(I)[3]) based on volume production model, curve-(II)[7]) with final state interaction (fsi) and curve-(II')[7]) without fsi.

(b) for ^{49}Cr : experimental results ; thin line-(a)[3]), thin line-(c)[2]) and thin line-(d)[6]) and theory ; curve-(I)[3]) based on surface production, curve-(I')[3]) on volume production model and circled crosses with error bars (but not given for σ_{225} from cascade-evaporation model[35]) calculated by[5,6]).

Fig. 4 Comparison of the total cross sections for $^{51}V(\gamma,\pi^- xn)$ reaction with the total photo-absorption cross sections approximated by the single nucleon total absorption cross section, $\sigma_{\gamma N}=(\sigma_{\gamma p}+\sigma_{\gamma n})/2$, multiplied by the target mass $A_t=51$.

KEY-WORD for CHROMIUM AND TITANIUM ISOTOPES PRODUCED IN PHOTONUCLEAR REACTIONS OF VANADIUM, REVISITED by K.Sakamoto

NUCLEAR REACTIONS $^{51}V(\gamma,\pi^+)$, $^{51}V(\gamma,\pi^-)$, $^{51}V(\gamma,\pi^-2n)$, $^{51}V(\gamma,\pi^-3n)$. Activation method. E_0=30-1000 MeV, measured σ_q. deduced σ_q for secondary $^{51}V(n,p)$ and (p,xn), σ_k for ^{51}Ti, ^{51}Cr, ^{50}Cr, ^{49}Cr and ^{48}Cr.

TABLE 1 Relevant nuclear data for yield measurements

Nuclide	Half-life	γ-Ray energy measured (keV)	Fractional abundance (%)
Ti-51	5.67 m	320.1	93.0
Cr-51	27.7 d	320.1	9.83
Cr-49	42.1 m	152.9	30.9
Cr-48	23.0 h	308.3	99.0
Na-24	15.02 h	1369.5	100
Au-196	6.18 d	355.7	86.9

TABLE 2 Measured yields of Titanium-51 and Chromium-51, 49 and 48 in unit of μb per equivalent quanta

End-point Energy, E_o (MeV)	Run	^{51}Ti	^{51}Cr	^{49}Cr	^{48}Cr	Chem. Yield (%)
1050	c (nd)	24.2 ± 0.9	—	29.5 ± 1.3	—	—
1000	a (nd)	28.0 ± 0.8	134 ± 17	30.5 ± 0.8	2.30 ± 0.59	—
	(ch)	—	—	—	2.25 ± 1.15	2.2
950	c (nd)	25.2 ± 1.3	—	30.6 ± 1.3	—	—
900	a (nd)	33.4 ± 5.1	134 ± 9	29.4 ± 1.3	1.39 ± 0.50	—
	(ch)	—	93 ± 56	—	1.17 ± 0.45	3.5
	b (nd)	—	—	24.4 ± 0.7	—	—
	(ch)	—	88.9± 6.5	—	2.57 ± 0.10	54.9
850	c (nd)	23.5 ± 1.9	—	26.2 ± 1.8	—	—
800	a (nd)	25.6 ± 3.0	108 ± 8	—	—	—
	(ch)	—	—	24.8 ± 7.3	1.89 ± 0.42	12.4
	b (nd)	—	—	23.8 ± 0.6	—	—
750	c (nd)	24.7 ± 1.8	—	22.5 ± 2.3	—	—
700	a (nd)	25.6 ± 3.4	127 ± 17	25.7 ± 1.0	2.83 ± 0.91	—
	(ch)	—	133 ± 4.3	—	2.92 ± 0.26	9.8
	b (nd)	26.0 ± 1.5	—	23.8 ± 0.6	—	—
	(ch)	—	107 ± 8	—	2.83 ± 0.05	48.1
650	c (nd)	21.7 ± 1.3	—	27.6 ± 1.6	—	—
600	a (nd)	24.1 ± 4.3	116 ± 14	24.2 ± 0.7	1.71 ± 0.45	—
550	c (nd)	25.1 ± 1.7	—	27.0 ± 2.8	—	—
500	a (nd)	36.4 ± 9.9	71.3± 7.8	20.5 ± 0.7	1.28 ± 0.56	—
	(ch)	—	120 ± 21	—	2.67 ± 0.23	21.1
	b(nd)	37.5 ± 5.6	—	20.9 ± 2.9	—	—
	(ch)	—	123 ± 54	—	2.27 ± 0.38	12.7
450	c (nd)	20.1 ± 1.6	—	22.8 ± 2.4	—	—
400	a (nd)	25.7 ± 5.0	68 ± 16	19.0 ± 1.6	1.92 ± 0.52	—
	(ch)	—	83 ± 39	—	2.66 ± 0.49	17.7
	b (nd)	—	—	18.9 ± 3.0	—	—
	(ch)	—	86 ± 38	—	2.16 ± 0.26	37.4
350	c (nd)	24.3 ± 3.7	—	15.0 ± 2.8	—	—
300	a (nd)	13.7 ± 3.0	—	15.8 ± 1.3	2.4 ± 1.0	—
	b (nd)	27.7 ± 4.4	—	16.5 ± 1.1	—	—
	(ch)	—	83 ± 26	—	1.38 ± 0.22	41.8
230	c (nd)	6.21± 0.23	46 ± 6.7	4.53 ± 0.19	—	—
	(ch)	—	—	4.31 ± 0.65	0.221± 0.035	59.5 ± 8.8
	d (nd)	—	86.6± 13.2	5.12 ± 0.27	—	—
	(ch)	—	52.5± 3.3	—	0.264± 0.048	38.7 ± 2.3

continued to page ii

End-point Energy, E_0 (MeV)	Run	^{51}Ti	^{51}Cr	^{49}Cr	^{48}Cr	Chem. Yield (%)
210	c (nd)	6.63 ± 0.23	73.5 ± 7.9	2.74 ± 0.07	—	—
	(ch)	—	47.1 ± 2.5	—	0.108± 0.016	28.9 ± 0.9
	d (nd)	7.21 ± 0.16	45.6 ±12.8	2.88 ± 0.10	—	—
	(ch)	—	34.2 ± 7.5	—	—	20.9 ± 0.9
175	d (nd)	2.21 ± 0.91	22.1 ± 1.3	0.313± 0.020	—	—
	(ch)	—	19.9 ± 1.5	—	(7.48±5.61) E-3	25.2 ± 0.8
150	d (nd)	—	13.0 ± 1.0	—	—	—
	(ch)	—	—	0.179± 0.016	(6.40±0.83) E-3	47.7 ± 4.2
149	a (nd)	1.8 ± 1.5	—	0.228± 0.028	—	—
	(ch)	—	24.4 ± 5.5	—	—	26.4 ± 5.2
125	d (nd)	1.60 ± 0.03	11.2 ± 1.0	0.162± 0.14	—	—
	(ch)	—	—	0.117± 0.013	(6.88±2.54) E-3	24.1 ± 2.4
120	c (nd)	3.546± 0.119	—	—	—	—
104	a (nd)	3.71 ± 0.76	—	—	—	—
65	a (nd)	3.1 ± 0.59	8.1 ± 2.7	—	—	—
	(ch)	—	—	(6.90±0.19) E-3	0 ±0.0006	29.1 ± 7.0
64	c (nd)	3.55 ± 0.12	—	—	—	—
55	c (nd)	3.5 ± 1.3	—	—	—	—
45	a (nd)	2.08 ± 0.09	—	—	—	—
	(ch)	—	8.75 ± 0.70	0 ± 0.0039	0 ±0.0005	25.4
40	c (nd)	1.10 ± 0.05	—	—	—	—
30	a (ch)	—	2.65 ± 0.29	0 ± 0.0010	0 ±0.0013	37.4

note : Results from triplicated runs a, b and c, are shown separately. The (nd) and (ch) indicate the non-destructive and radiochemical measurements, respectively. For the latter, the chemical yields of chromium are shown.

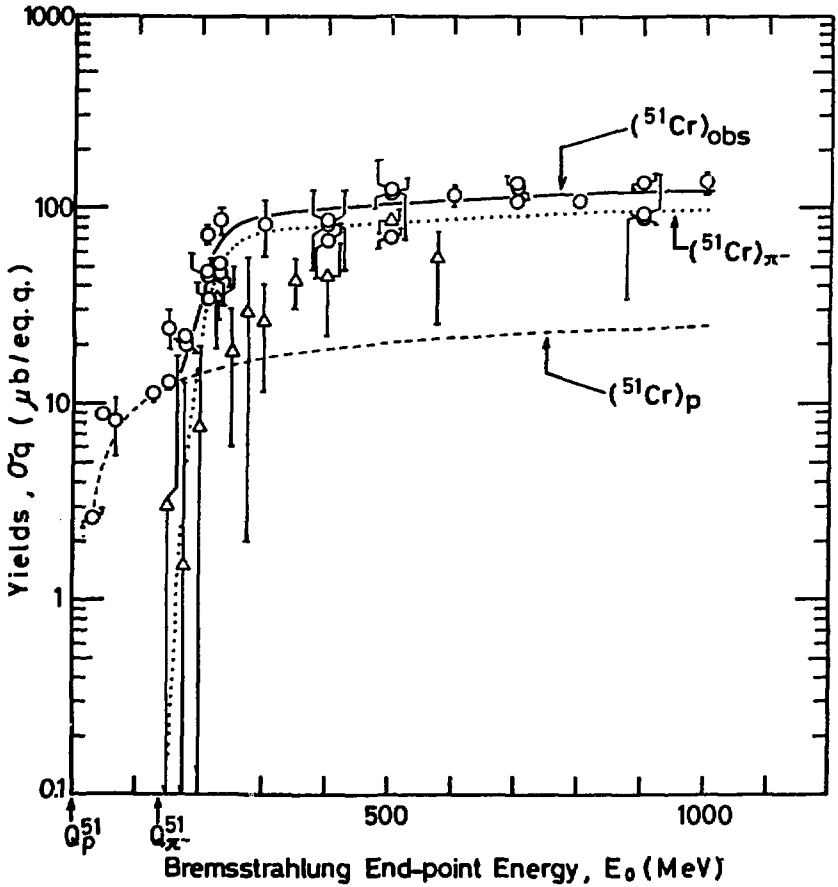
1000
100
10
1
0.1
Yields , σq (μb/eq.q.)
(51Cr)obs
(51Cr)π-
(51Cr)p
500
1000
Q51p
Q51π-
Bremsstrahlung End-point Energy, E0 (MeV)

Fig. 1(a)

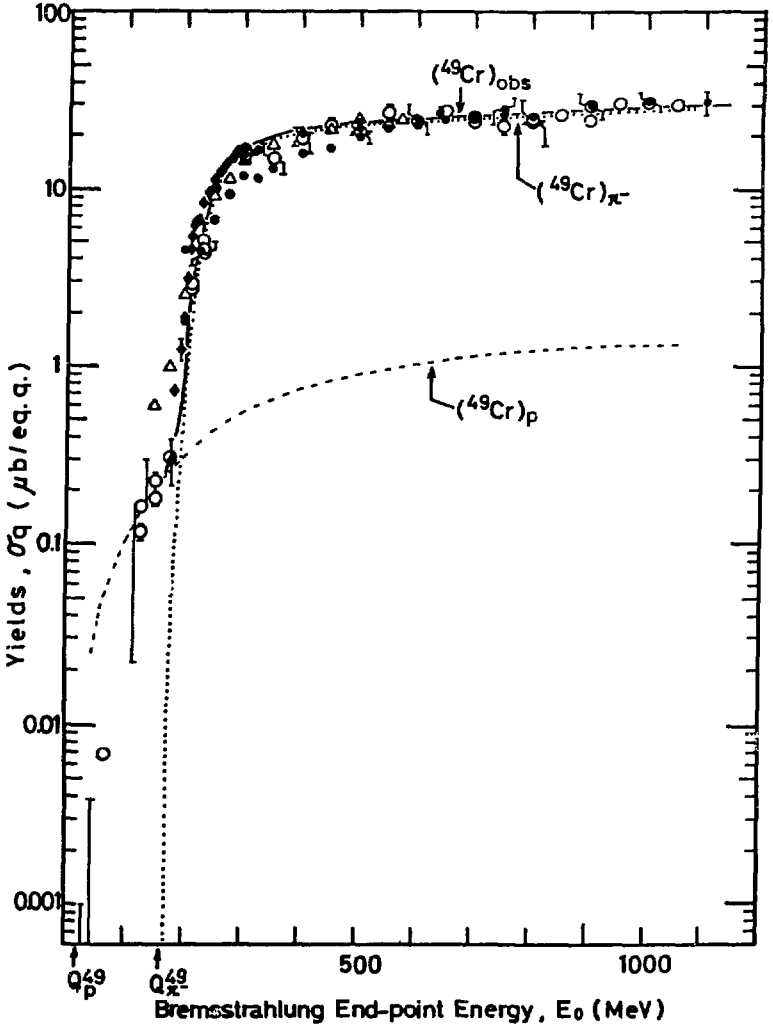
100
10
1
0.1
0.01
0.001
Yields, σq (μb/eq.q.)
(49Cr)obs
(49Cr)π-
(49Cr)p
Qp49
Qπ-49
500
1000
Bremsstrahlung End-point Energy, E0 (MeV)

Fig. 1(b)

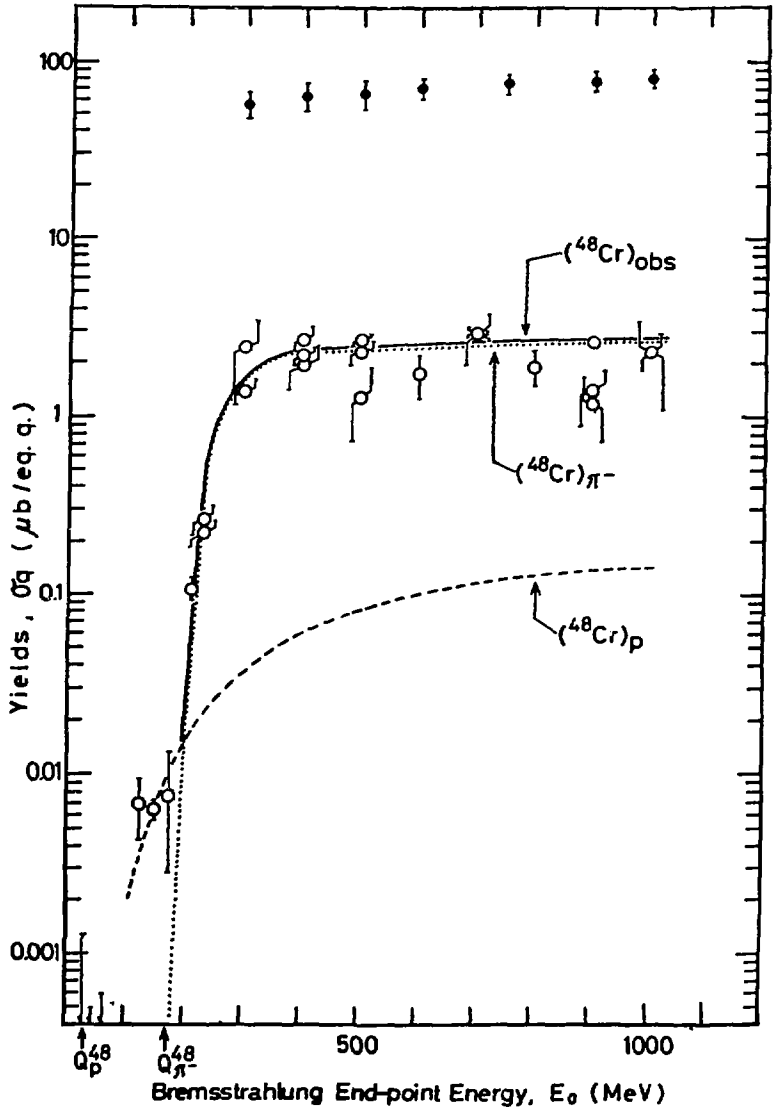
100
10
1
0.1
0.01
0.001
Yields, σq (μb/eq. q.)
(48Cr)obs
(48Cr)π-
(48Cr)p
Q48p
Q48π-
500
1000
Bremsstrahlung End-point Energy, Eo (MeV)

Fig. 1(c)

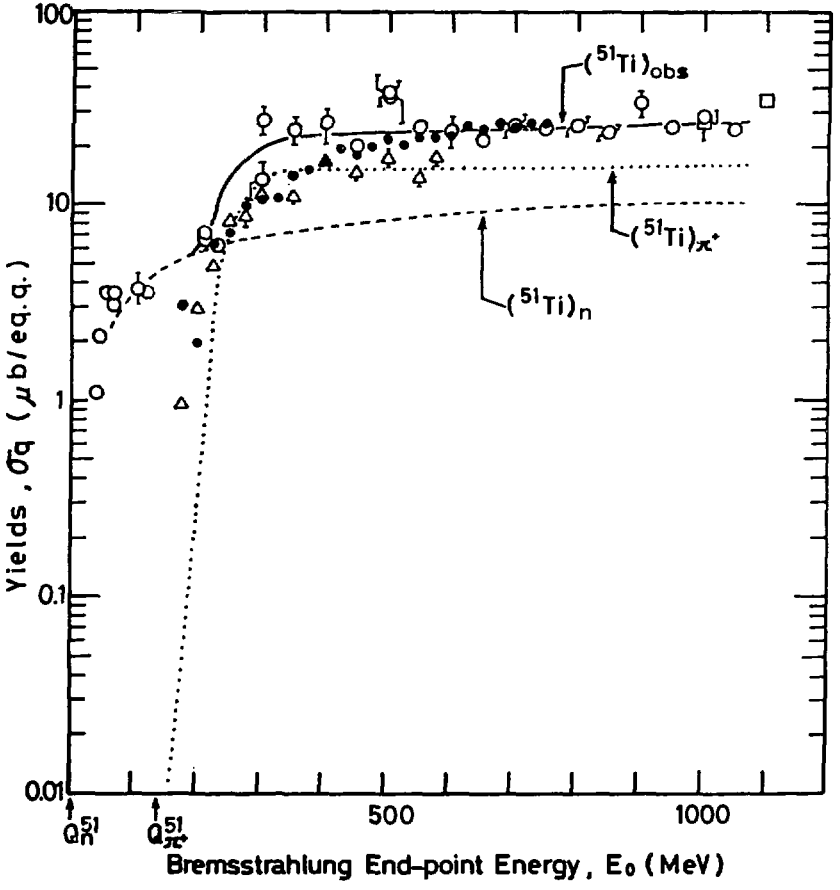
100
10
1
0.1
0.01
Yields , σq (μb/eq.q.)
(51Ti)obs
(51Ti)π+
(51Ti)n
500
1000
Bremsstrahlung End-point Energy , E0 (MeV)

Fig. 1(d)

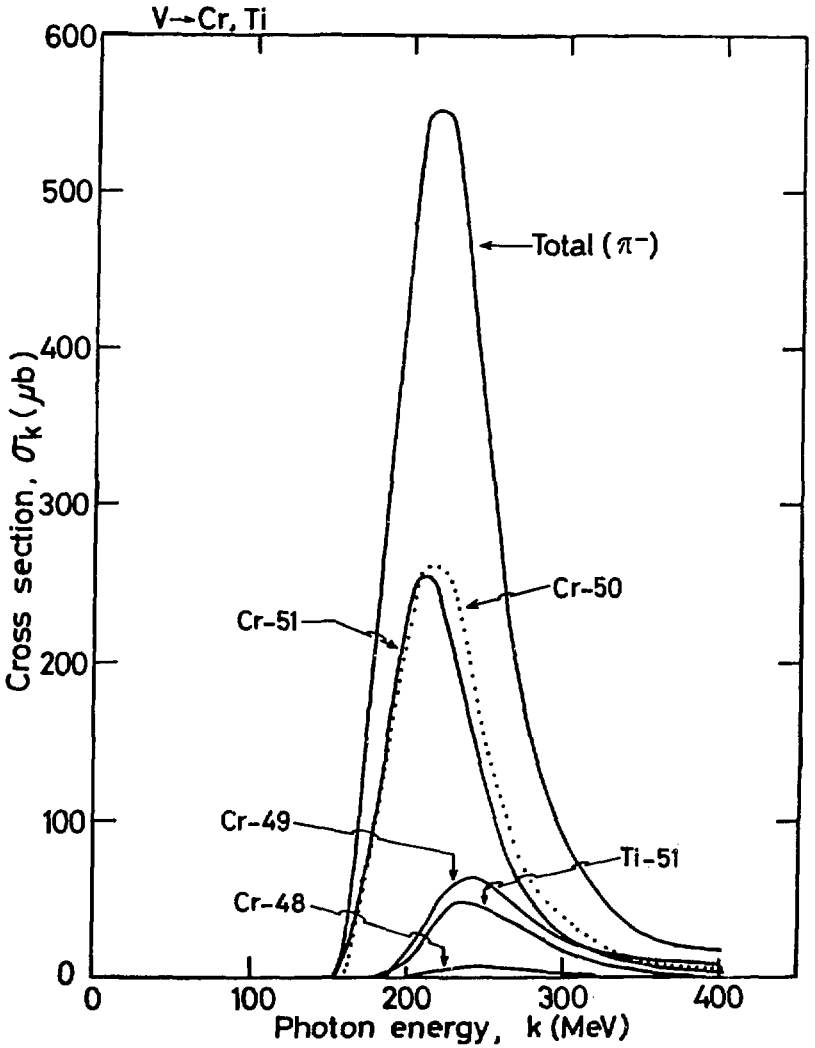
V→Cr, Ti
600
500
400
300
200
100
0
Cross section, σ_k (μb)
Total (π^-)
Cr-50
Cr-51
Cr-49
Ti-51
Cr-48
0
100
200
300
400
Photon energy, k (MeV)

Fig. 2

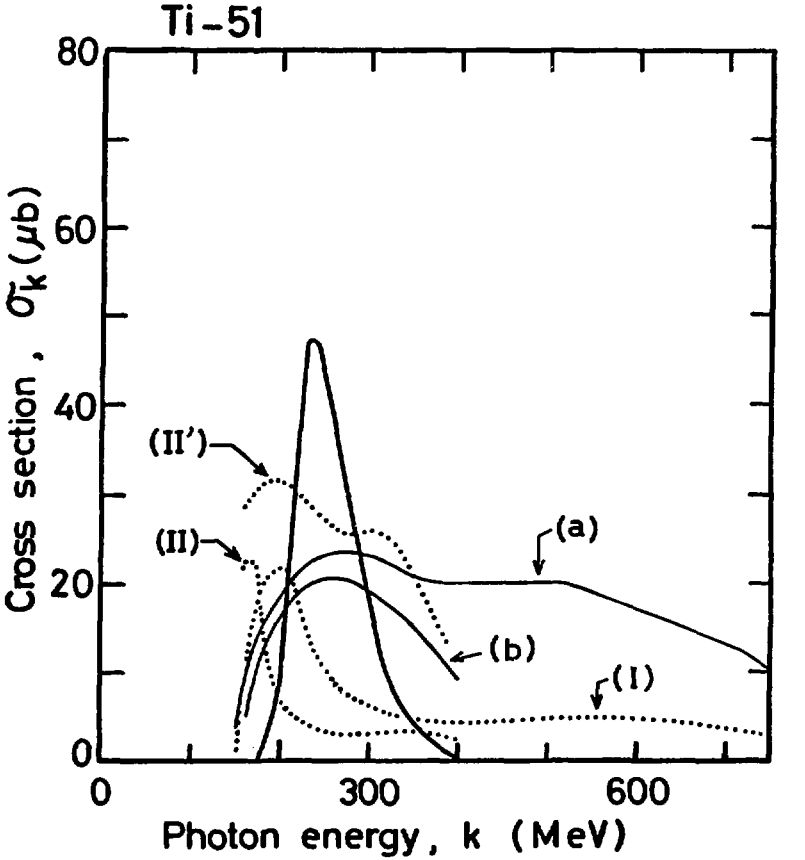
Ti-51
80
60
40
20
0
Cross section, σ_k (μb)
(II')
(II)
(a)
(b)
(I)
0
300
600
Photon energy, k (MeV)

Fig. 3(a)

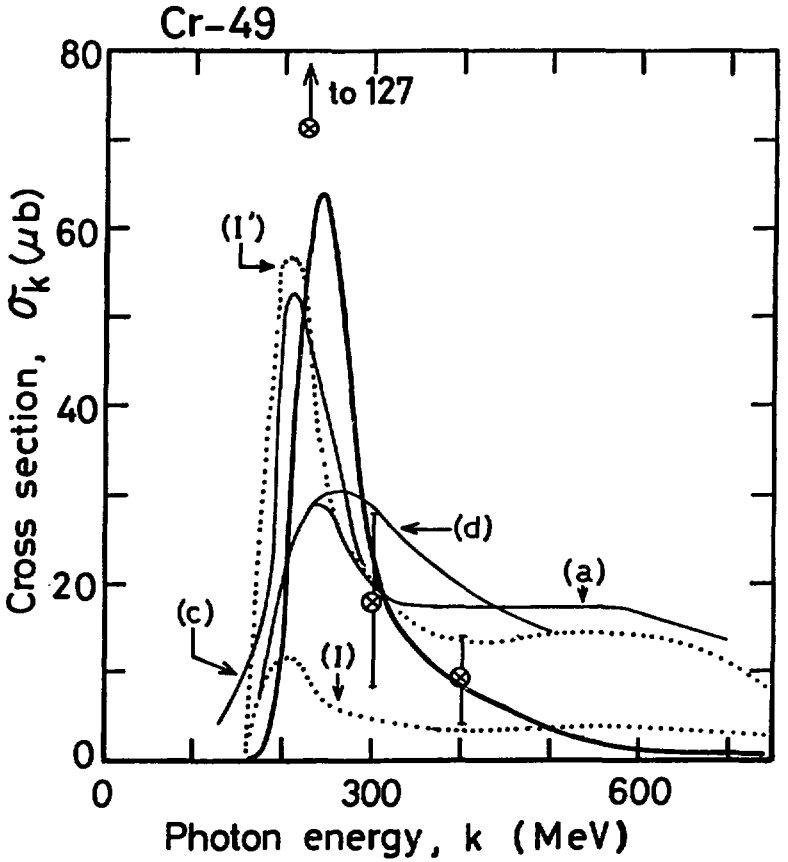
Cr-49
80
60
40
20
0
to 127
(I')
(d)
(a)
(c)
(I)
0
300
600
Photon energy, k (MeV)
Cross section, σ_k (μb)

Fig. 3(b)

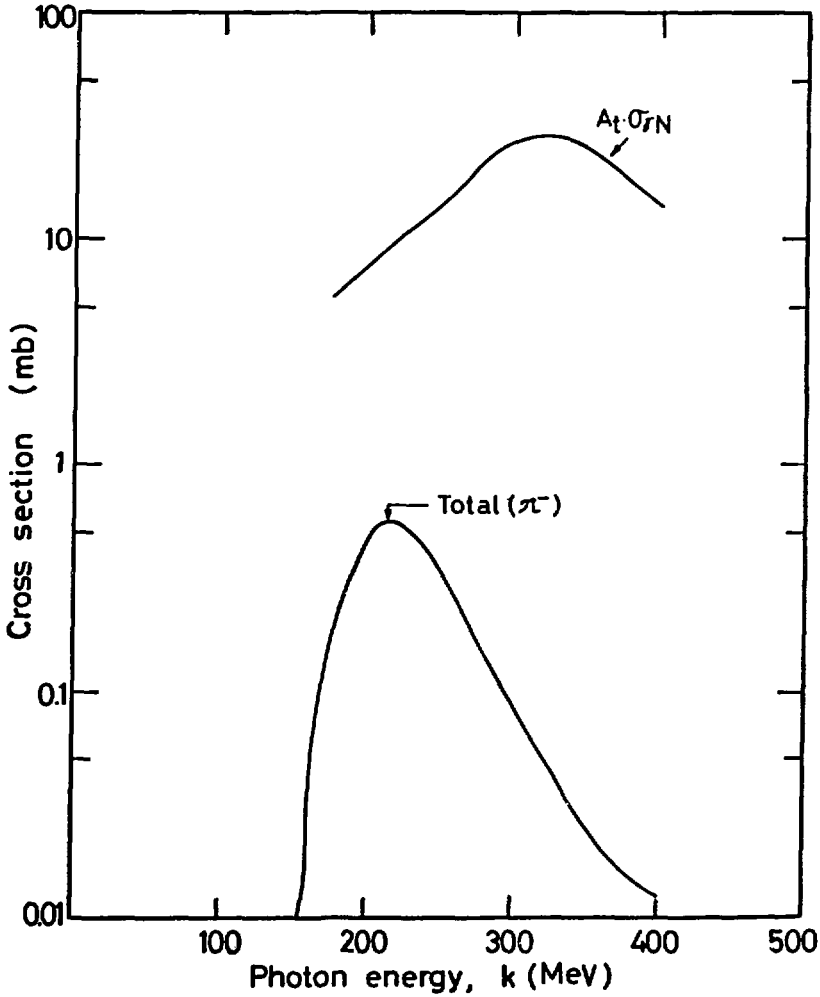
100
10
1
0.1
0.01
Cross section (mb)
$A_t \cdot \sigma_{\gamma N}$
Total (π^-)
100
200
300
400
500
Photon energy, k (MeV)

Fig. 4